From spin fields to galaxy gravity

A force law from the ESFD equations

Christopher Grenke's clock law couples elapsed time to the local spin–field contraction. His spin–entropy equation assigns gravitational mass density to the divergence of a collective current. Taken together, they allow two different questions to be tested. Can the measured magnetic field supply the missing radial force? Can a collective spin response produce the force even where a local magnetic field has little radial gradient?

The collective calculation gives a specific prediction. If the reversible quartic spin coordinate carries the current, responds to the gravitational potential gradient, and has the critical susceptibility derived on page 3, the spherical acceleration is

$$g = g_b + (a_q^2\, g_b)^{1/3}.$$

Here g_b is the Newtonian acceleration of the observed baryons and a_q is one common acceleration scale. Far outside an isolated finite mass, this model predicts a 12% increase in speed each time the radius doubles. That exponent follows from the quartic energy. The identification of a spin current and the value of its susceptibility are physical assumptions.

Test	Result
Five independent radio profiles	The direct magnetic prediction raised the held-out equivalent-speed error from 48.6 to 56.5 km/s relative to baryons alone. One galaxy required the opposite sign.
376 archived rotation curves	The collective quartic law reduced the galaxy-weighted speed error from 55.3 to 21.8 km/s in SPARC and from 74.1 to 40.6 km/s in external PROBES. Other gravity laws gave comparable errors.
NGC 2403	With the entire galaxy held out of calibration, the quartic law reached 7.24 km/s RMS error across 73 measured radii. It predicted 128.4 km/s at the last point, where the measured speed was 134.0 km/s.

The data favor a collective acceleration tied to the baryonic distribution over an extra force proportional to the gradient of the measured field squared in these tests. They leave open whether the collective response is carried by spin. That identification requires physics beyond rotation-curve fitting.

ESFD manuscripts · 21.docx §3.2, 4.1.docx §§11.2–11.3, November master §9, and the 27 November spin-response revision. Galaxy inputs · SPARC, PROBES and LOFAR.

How a spin-dependent clock could produce attraction

The clock branch in 21.docx gives $\Phi_{EM} = \kappa_{EM} S_{\mu\nu} F^{\mu\nu}$ and $d\tau = \exp(-\xi\Phi_{EM})\, dt$. The earlier 4.1.docx also gives an exponential clock law and motivates gravity through $F = T\nabla S$. Use the dimensionless quantity $u = -\ln(d\tau/dt)$ for a clock at rest. Treating that rate as the lapse N of a stationary metric common to all matter, and assuming geodesic free fall, gives the weak, slow-motion limit

$$\Psi = c^2 \ln N = -c^2 u,\ a = -\nabla\Psi = c^2\nabla u,\ v_c^{\,2} = -c^2\, du/d\ln R.$$

A larger u near the center therefore gives an inward acceleration. A shift confined to one clock transition would require different physics. Universality is essential. The printed coefficients in the draft's clock example do not supply a measured universal coupling.

An explicit inverse-square solution

Promote u to an independent collective amplitude. Let u_B denote its preferred local spin–magnetic part. Give gradients of $u-u_B$ a stiffness K and couple rest mass density ρ_b to the same lapse. One trial static energy is

$$E = \int [\ \tfrac{1}{2}K\,|\nabla(u-u_B)|^2 + \rho_b c^2\,(e^{-u}-1)\ ]\, d^3x.$$

With fixed u_B and fields vanishing at infinity, stationarity gives $\nabla^2(u-u_B) = -(\rho_b c^2/K)e^{-u}$. At first order, a point mass M gives $u-u_B = G_{eff}M/(c^2 r)$, where $G_{eff} = c^4/(4\pi K)$. The gradient yields the ordinary inward force per unit mass, $G_{eff}M/r^2$. Matching measured G requires $K = 9.63 \times 10^{42}$ N. This calibrates a stiffness. Its microscopic value and the universal coupling to neutral mass remain to be derived.

The same equation supplies the ordinary baryonic potential used in the radio test. Its extra effective density is $\rho_x = -(K/c^2)\nabla^2 u_B = \nabla\cdot Q$ with $Q = -(K/c^2)\nabla u_B$, in kg/m². A strictly local identity $u = \xi\kappa_{EM} S\cdot F$ leaves no independent mode to vary. Introducing the collective degree of freedom adds that missing assumption. A finite correlation length λ, modeled by $K(u-u_B)^2/(2\lambda^2)$, would cut off the point-source field as $\exp(-r/\lambda)/r$.

Author's clock and entropy proposals · 21.docx §§3.2–3.3 and 4.1.docx §§11.2–11.3. The energy, stiffness matching and weak-field derivation on this page are proposed here.

The quartic spin response fixes an outer slope

Start independently from the November master's $\rho_x = \nabla\cdot Q$, with Q proportional to its entropy-weighted spatial current sJ_s. Its weak-field Poisson equation is $\nabla\cdot(\nabla\Psi - 4\pi G Q) = 4\pi G\rho_b$. In a regular spherical configuration define the positive outward gradient $g = \partial\Psi/\partial r$ and $y = 4\pi G Q_r$. Integration on a sphere gives $g - y = GM_b(<r)/r^2 = g_b$. Test bodies accelerate inward. Both g and y have acceleration units.

The previous revision's reversible spin coordinate obeys $ap + bp^3 = h$, with $a,b > 0$ and measured drives in principle from field or rotation. Try a gravitational matching $h = \lambda g$ and $y = \kappa p$ with positive alignment. Eliminating p gives $g = A\,y + y^3/a_q^{\,2}$, with $A = a/(\lambda\kappa)$ and $a_q^{\,2} = \lambda\kappa^3/b$. This new drive and current identification require a microscopic justification.

> $g_b = (A-1)y + y^3/a_q^{\,2}$. At $A = 1$, $g = g_b + (a_q^{\,2} g_b)^{1/3}$.

Both static equations follow by varying one energy. Write y as a vector parallel to the equilibrium spin current. At A = 1 the energy density is $\rho_b\Psi + [\tfrac{1}{2}|\nabla\Psi - y|^2 + |y|^4/(4a_q^{\,2})]/(4\pi G)$. Varying Ψ gives the weighted-current Poisson equation. Varying y gives $\nabla\Psi = y + |y|^2 y/a_q^{\,2}$. Its two field-energy terms are nonnegative. Replacing the quartic term with $|y|^3/(3a_c)$ gives the cubic-energy alternative below.

For $A > 1$ the weak-source response is asymptotically proportional to g_b. $A = 1$ cancels the linear term and exposes the nonlinear spin response. This is a tuned critical susceptibility. For an isolated finite mass in the regime $y \gg g_b$, the extra circular speed obeys $v_x^{\,6} = GMa_q^{\,2}r$ and the total speed approaches the same $r^{1/6}$ scaling. An indefinitely flat rotation curve would contradict this asymptote in that regime.

Two flat-speed comparisons

Changing the leading nonlinear spin energy to $|p|^3$ gives a signed $p|p|$ term in the response. With the same critical matching, $g - y = y^2/a_c$ for $y \geq 0$. Thus $g = g_b + \sqrt{(a_c g_b)}$, giving $v_x^{\,4} = GMa_c$ outside the mass. This change to the spin energy is a candidate modification. The analytic p^4 term alone gives the other exponent.

A separate control takes $4\pi GQ = [1 - \mu(g/a_s)]\nabla\Psi$, with $\mu(x) = x/(1+x)$. The divergence equation becomes the AQUAL modified Poisson equation. In spherical symmetry $g = [g_b + \sqrt{(g_b^{\,2} + 4a_s g_b)}]/2$. Its flat limit gives $v^4 \to GMa_s$. This is the established simple MOND interpolation. Its success cannot distinguish an ESFD current from an equivalent force law.

Extended indefinitely, the quartic excess potential grows as $r^{1/3}$ and the flat-speed potentials as $\ln r$. A global solution with finite lapse needs an environmental boundary or a further change in the response. The data below probe finite radii.

ESFD · November master §9 and research/spin_response. Nonlinear potential theory and the simple interpolation · Bekenstein & Milgrom (1984) and Famaey & Binney (2005).

A direct test with measured magnetic fields

In a magnetic rest frame with negligible electric terms, choose the spin convention S:F = 2 s·B. For weak, aligned spin response at fixed susceptibility and negligible rotation drive, $p \propto B$, so $u_B = qB^2$. Define $C = c^2q$. The local excess in squared circular speed is $-C\, dB^2/d \ln R$. A uniform magnetic field supplies zero extra radial force. A constant extra speed over a radial interval requires B^2 to fall linearly with $\ln R$ there.

$$\int (v_{obs}^2 - v_b^2)\, d \ln R = C\,[B^2(\text{inner}) - B^2(\text{outer})].$$

This integral uses the potential difference directly and avoids differentiating a noisy digitized field profile. The right side comes from radio observations. The left side comes from the rotation curve and its baryonic decomposition. Annular equipartition strengths approximate the spin-weighted field. In particular, squaring an annular mean and averaging the true local B^2 are different operations.

We rescaled radio radii to each SPARC distance. Of 201 archived radio rings, 183 lie within the native rotation curves. At each radius we integrated a piecewise-linear interpolant of squared speed in $\ln R$. We averaged the integral and B^2 over the first and last quarters of retained rings, then divided the contrast by the separation of their mean log radii. The square root of the resulting mean v^2 is the interval-equivalent speed. Each row below is one galaxy.

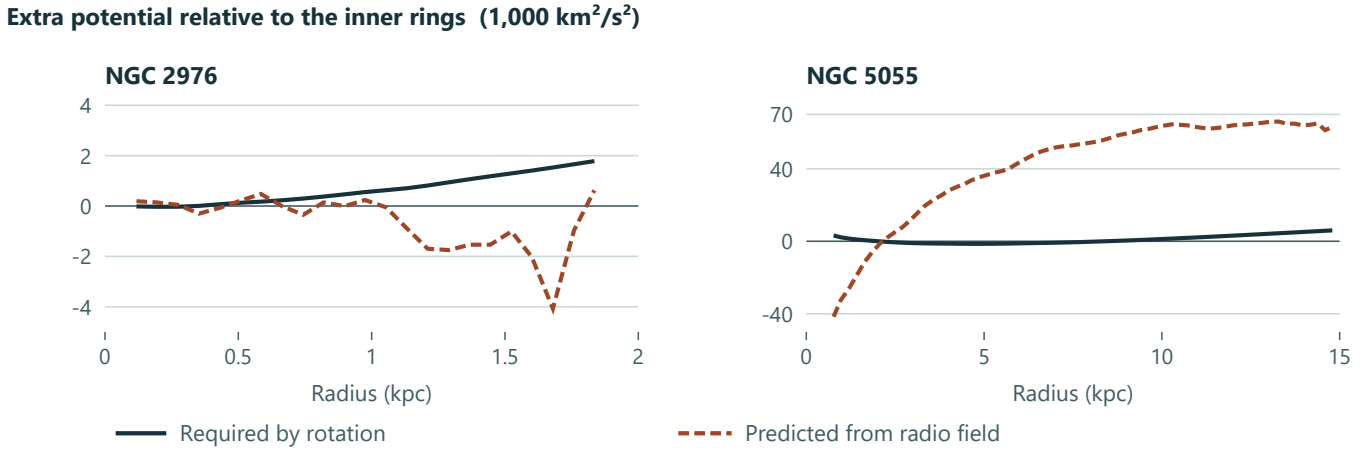
Galaxy	Inner → outer field, μG	Observed speed, km/s	Magnetic + baryons, km/s
NGC 2841	8.42 → 7.58	315.4	217.6
NGC 2976	9.58 → 10.39	44.0	18.8
NGC 3198	10.71 → 8.61	94.2	80.0
NGC 5033	15.28 → 8.51	220.1	199.1
NGC 5055	17.53 → 8.27	195.1	266.7

Each prediction used a single nonnegative C fitted on the other four galaxies. Each field value shown is the root mean square of the published annular estimates in its endpoint group. Folds used unweighted squared-speed loss across galaxies. Correlated rings share photometry, geometry and interpolation. They do not provide 183 independent tests.

Radio field estimates · Heesen et al. (2023), Appendix D. Kinematics and mass models · Lelli, McGaugh & Schombert (2016). Matched inputs and digitized rings are in the release.

Where the magnetic prediction fails

The sign mismatch occurs in NGC 2976. The equivalent baryonic speed is 33.7 km/s and the measured value is 44.0 km/s, requiring extra inward acceleration on average. The rise in field strength gives an outward contribution. In NGC 5055 the field falls steeply and predicts too much acceleration. In NGC 2841 the field falls too little for the large required excess.



The solid curve is the integrated excess potential from rotation. The dashed curve uses the field and the coefficient fitted on the four other galaxies. Each is referred to its own inner-group mean. The panels have different vertical scales. Zero extra field-induced potential at all radii would track NGC 5055 more closely than the held-out prediction.

Prediction	RMSE of equivalent v^2, km²/s²	RMSE of equivalent speed, km/s
Baryons alone	24,590	48.6
Baryons + magnetic term	27,912	56.5
Baryons + constant excess v^2	24,562	65.3
Previously calibrated cored law	15,688	29.9
Local spin term alone	51,275	138.0 over 4 valid speeds

The local-only law gives negative v^2 for NGC 2976. The other rows have five valid speeds. Changing the magnetic response from B^2 to the full quartic crossover at 10 μG or to $B^{4/3}$ gives 58.1 and 58.6 km/s. Unrestricted signs leave the primary fit unchanged. Fractional-error refitting gives 49.5 versus 48.6 km/s for baryons. Tightening the allowable native radial gap to 1.5 kpc leaves four galaxies and raises magnetic error to 182.5 km/s. The small sample is sensitive to radial coverage and weighting.

On exactly these five intervals, the collective quartic, cubic and simple MOND predictions give 31.0, 29.4 and 31.2 km/s, respectively. Each used 105 other SPARC galaxies for training. The magnetic fits had four other galaxies with independent field profiles.

Tables · magnetic_scores.csv, magnetic_folds.csv, magnetic_profiles.csv and magnetic_profile_errors.csv. The radio error bars in the source describe annular scatter. No significance level is assigned to these five-galaxy contrasts.

Rotation-curve tests across 376 galaxies

Each collective model used one acceleration scale. For SPARC, that scale was fitted on four archived galaxy folds and predictions were scored on the fifth. For the external test, each scale was calibrated once on all 131 SPARC galaxies and frozen on 245 PROBES galaxies. No observed velocity from a scored galaxy entered its collective force prediction. The analysis used 3,032 distinct galaxy–radius pairs from SPARC and 15,976 from PROBES. Repeated radii were combined in squared speed.

Force law	SPARC · 131 galaxies	PROBES · 245 galaxies
Baryons alone	55.30 / 44.73	74.08 / 64.82
Critical quartic spin energy	21.76 / 14.20	40.64 / 30.93
Critical cubic spin energy	22.63 / 12.78	38.07 / 28.96
Simple MOND interpolation	21.30 / 13.04	39.31 / 29.80
Archived cored law	21.52 / 12.45	39.56 / 29.92

All figures are km/s. The first number is the square root of the equally weighted mean of the galaxies' mean squared velocity errors. The second is the median per-galaxy RMS error. Both use each galaxy's full sampled curve. The earlier inner-anchored outer-disk experiment asked a different question and used different errors.

The full-SPARC acceleration scales were 4.83×10^{-11} m/s² for the quartic law, 6.40×10^{-11} m/s² for the cubic law and 1.10×10^{-10} m/s² for simple MOND. Quartic spin improved on baryons in 123 of 131 SPARC and 239 of 245 PROBES cases. It beat the archived cored law in 58 and 85, respectively. The cubic-energy modification beat quartic in 174 external galaxies and had the lowest external average error here. In SPARC its average error was the largest of the three collective laws.

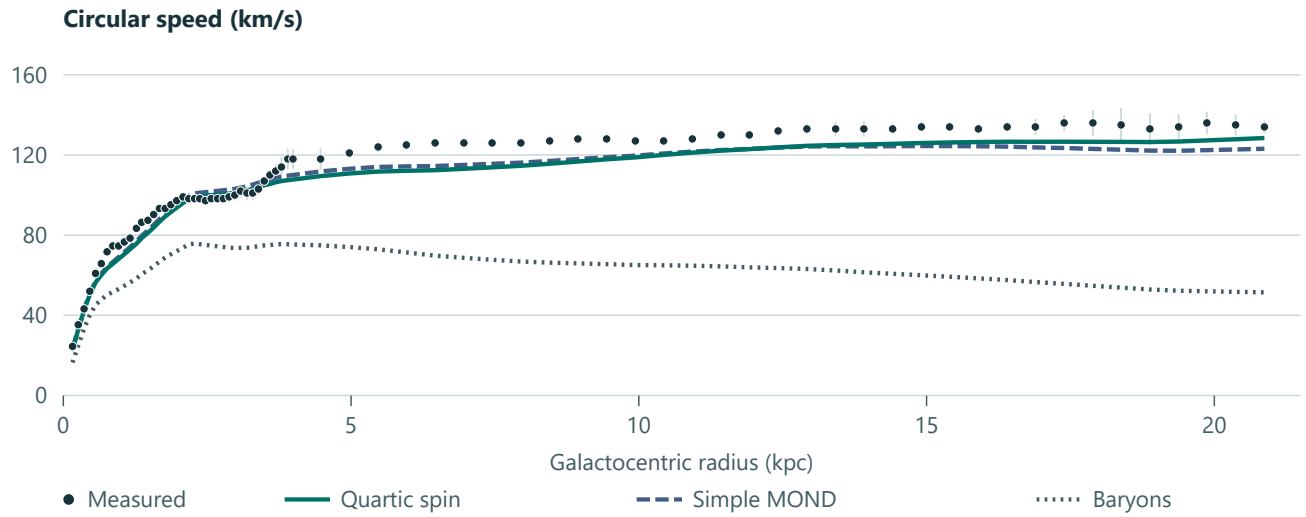
Scope of the disk calculation

The radial formula is exact in spherical symmetry. For disks we substituted $g_b = v_b^2/R$ using the archived disk baryon model. A full nonlinear field solution requires the three-dimensional mass and boundary conditions. PROBES uses approximate exponential stellar and gas disks and redshift-based distances. Gas distribution, inclination and stellar mass uncertainties affect the absolute errors. These common inputs let the data distinguish some response laws without identifying their microscopic source.

SPARC mass models · PROBES I data · Archived external sample selection, folds and baryon models. Reproducible outputs · collective_galaxies.csv and collective_scores.csv.

NGC 2403 gives a concrete field target

The quartic law fitted without NGC 2403 gives $a_q = 4.92 \times 10^{-11}$ m/s² and an RMS error of 7.24 km/s over its 73 radii. Simple MOND gives 7.46, the cubic modification 10.63, the archived cored law 11.08 and baryons alone 50.70 km/s. The quartic prediction at 20.87 kpc is 128.44 km/s, compared with 134.0 ± 3.12 km/s observed. This local agreement coexists with weaker quartic performance across the external sample.



An independent way to check the magnetic explanation

From 10.435 to 20.87 kpc the measured curve requires an extra potential rise I = 9,770.6 km²/s² beyond baryons. The implied inner-minus-outer spin lapse is $I/c^2 = 1.087 \times 10^{-7}$. As a clock signal that would correspond to 32.6 m/s in equivalent redshift after separating baryonic, kinematic and other contributions. This is an inferred target from rotation.

The five-galaxy retrospective fit gives C = 91.54 (km/s)²/μG². At that value the weak magnetic law requires $B^2(10.435\ \text{kpc}) - B^2(20.87\ \text{kpc}) = 106.7\ \mu\text{G}^2$. Even zero outer field requires an inner field of at least 10.33 μG. The four-galaxy values of C range from 61.64 to 268.77, so this target depends strongly on calibration. The archive's 5.7 μG value is a disk mean. Sparse line-of-sight Faraday data do not establish either annulus's total field. A radially resolved measurement across both annuli would test the stated requirement.

SPARC kinematics and Chyży et al. (2017), disk field. Curve and integral · NGC2403_curve.csv and outer_lapse_targets.csv. Error bars in the chart are the archived SPARC speed errors.

Does the same field bend light?

A clock gives the temporal potential Ψ. Weak lensing also depends on the spatial potential Φ, through $(\Psi+\Phi)/2$ in the convention with spatial metric $(1-2\Phi/c^2)\delta_{ij}$. A purely conformal metric $e^{-2u}\eta_{\mu\nu}$ gives $\Phi = -\Psi$ and zero light deflection in this isolated weak-field construction. The archived late-type galaxy stacks have nonzero shear, with inferred circular speeds of 130.2–267.7 km/s across the 24 cells used here. Pure conformal rescaling on flat spacetime fails as the sole origin of that lensing.

A second trial completion sets $\Phi = \Psi$. Then the shear-inferred circular acceleration is the one predicted by the radial force law under spherical isolation. For each of four published baryonic mass bins, we treated its tabulated mass as compact at 50–300 kpc, used the SPARC-calibrated acceleration scales, and made predictions at all six available radii. This adds a metric assumption while introducing no fitted lensing parameter.

Model for nonzero lensing	RMS against 24 tabulated speeds
Compact Newtonian baryons	139.3 km/s
Quartic spin, equal potentials	37.8 km/s
Cubic spin, equal potentials	33.8 km/s
Simple MOND, equal potentials	24.1 km/s

A direct look at radial shape

Between inner and outer pairs of lensing radii, the observed logarithmic speed slopes are +0.006, +0.182, +0.074 and −0.174 in order of increasing bin mass. Quartic spin predicts +0.155, +0.140, +0.126 and +0.106. It requires a rise in all four bins over this range. The observed slopes vary in sign. Projection, bin mass distributions, possible extended gas, environment and inter-bin covariance limit the comparison. These unweighted errors and slopes are descriptive.

The data require a source of light deflection. The spin-dependent clock supplies no equation for Φ. Equal potentials work appreciably better than the purely conformal choice in this test, but a causal relativistic spin theory still has to derive the spatial response.

Mistele et al. (2024), isolated-galaxy lensing. Source table 1, LTG mass bins, 62.71–291.07 kpc within the chosen 50–300 kpc window. Results · lensing.csv and lensing_slopes.csv.

What the measurements now demand of ESFD

A collective carrier. Ordinary attraction follows conditionally from a long-range spin mode with positive stiffness and a rest-mass coupling. The microscopic theory would have to derive the coupling for neutral, unpolarized matter, identify the current Q and determine whether its linear susceptibility reaches the critical value. A fit to rotation fixes one scale in each model. It does not measure any of these three ingredients.

A decision about the outer force. Quartic spin gives a rising outer speed around an isolated finite mass. A leading $|p|^3$ energy gives a flat outer speed and performed better on the external rotation curves. The two predictions can be separated with independently measured baryon mass profiles and extended dynamical or lensing radii. The near-flat limit of the cubic law also has a characteristic high-acceleration transition different from simple MOND. A physical spin sector must explain the form of its energy and its range of validity.

A measured field gradient. The five galaxy-specific values of C required by the radio test are +3,761, −95, +254, +170 and +18 $(km/s)^2/\mu G^2$ in the order on page 4. A single common coefficient misses both the sign and the range of amplitudes. Density-dependent susceptibility, differences between ordered and turbulent fields, or a rotation-driven response remain possible. Each would require an independently constrained spin model or observable. Fitting a separate C to each galaxy would remove the prediction being tested.

A target for additional galaxies. We integrated the outer radial half wherever at least three distinct measured radii cover that part of a curve. All 129 eligible SPARC galaxies and 243 of 245 eligible PROBES galaxies require a positive extra potential difference. The median required inner-minus-outer u is 7.18×10^{-8} and 1.38×10^{-7}, respectively. Two short SPARC outer curves miss the sampling rule. These values specify the sign and amplitude that future independent spin measurements must reproduce.

Reproducing the study

The research bundle contains the seven input tables, the method specification, the analysis and checks, all thirteen derived result files, and this manuscript and its rendering source. Run **python research/spin_gravity/checks.py** from its extracted root. The checks regenerate the numerical results, verify radial integration and force identities, recover known synthetic scales, and check that a held-out galaxy's velocities cannot set its magnetic prediction.

Project provenance · recovered 21.docx and 4.1.docx, November master §9, and Pattern Nexus ESFD research archive. Numerical provenance and the timing of exploratory choices · research/spin_gravity/README.md.